SynOpen K. K. Goel et al. THIEME OPEN ACCESS Paper

Design, Synthesis and Biological Evaluation of Imidazole-Substituted/Fused Aryl Derivatives Targeting Tubulin Polymerization as Anticancer Agents

Kapil Kumar Goel *[a,b]
Satyendra Kumar Rajput[a]
Rajeev Kharb *[b]

[a] Department of Pharmaceutical Sciences, Gurukul Kangri (Deemed to be University), Haridwar-249404, India
kapilgoel@gkv.ac.in
[b] Amity Institute of Pharmacy, Amity University, Sector 125, Noida, Uttar Pradesh 201301, India
rajeevkharb_2007@rediffmail.com

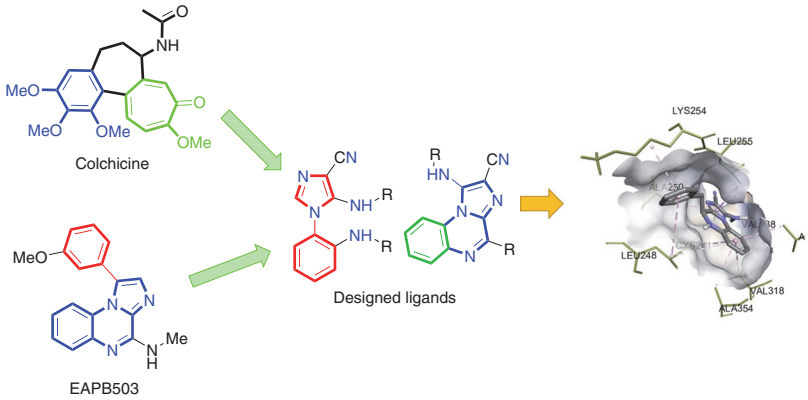

Received: 18.10.2022
Accepted after revision: 14.12.2022
Published online: 26.01.2023 (Version of Record)
DOI: 10.1055/s-0042-1751835; Art ID: SO-2022-10-0054-OP

Abstract The development of new pharmacologically active molecules targeting tubulin polymerization has recently attracted great interest in research groups. In efforts to develop new potent anticancer compounds, imidazole-tethered/fused pharmacologically active aryl derivatives possessing different substitution patterns targeting tubulin polymerization have been rationally designed and synthesized. The target molecules (P1-5 and KG1-5) were synthesized by multistep syntheses involving the reaction of intermediate 2-aminophenyl-tethered imidazoles with appropriate reactants in the presence of *p*-TsOH under different conditions. The synthesized compounds displayed moderate to good cytotoxicity, comparable to that of colchicine, against four cancer cell lines (MCF-7, MD-MBA-231, A549, and HCT-116). Compounds P2 and P5, with an imidazoloquinoxaline moiety, emerged as potential leads with cytotoxicity profiles against these cell lines similar to colchicine. Compounds P2 and P5 arrested cell division at the G2/M phase and prevented cancerous cell growth through induced apoptosis. These results favored the hypothesis that the compounds might act by binding to the colchicine binding site, which was further confirmed with the help of a tubulin polymerization inhibition assay. The results encourage the further exploration of imidazoloquinoxalines as promising leads that deserve advanced clinical investigation.

Key words imidazoloquinoxalines, anticancer agents, tubulin, imidazoles, cytotoxicity, cell division, drug design

Introduction

Cancer has been one of the most severe health ailments worldwide for the last few decades, with millions of deaths every year.[1] It is estimated that around 19.3 million new cases and 10.0 million deaths were reported in 2020 alone.[2] Abnormal gene functioning and mutated gene expressions play a significant role in cancer progression. There are several hallmarks associated with cancer cells, such as tissue invasion, metastasis, apoptosis, and angiogenesis.[3] These hallmarks were put forth as significant target approaches for the development of new anticancer drug molecules. From the identified targets against cancer, tubulins (α- and β-tubulin heterodimers) are widespread cytoskeleton parts that play a vital role in cell division, signaling, and the maintenance and development of cells.[3] A dynamic equilibrium is maintained between the α- and β-tubulin heterodimers and microtubules, forming the protofilaments. During the mitosis phase of cell division, this helps to correct chromosome segregation caused by mitotic spindle formation failure, which can cause cell cycle arrest.[4] In various types of cancer, tubulin expression is altered, which leads to fast cell growth and tumor formation.[5] Drug molecules targeting this tubulin–microtubule equilibrium state stop the cell division process at the metaphase–anaphase transition phase, causing mitochondrial apoptosis or cell death.[3,6] For decades, various research groups have been directly or indirectly involved in the quest to develop or find new anticancer molecules. There are many libraries of synthetic and natural compounds that are being explored against cancer targets possessing a wide range of structural features and parameters.[7] The tubulin polymerization inhibitor colchicine is one of the most significant drug molecules that act by binding at the junction of the α- and β-tubulin monomers in the polymerized form to arrest the cell cycle.[8] However, colchicine's low safety window and dose-related toxicity have limited its clinical use.[9] Various structurally modified chemical moieties related to colchicine and combretastatin have since come under investigation.[10]

Current research is exploring a wide range of N-heterocycles, either fused or non-fused, as potential anticancer agents.[11] Imidazole-linked aryl derivatives (non-fused imidazole derivatives) and imidazoloquinoxaline (fused imidazole derivatives), also named imiqualines, are critical structural features containing imidazole scaffolds with a wide range of pharmacological activities, such as anticancer, rheumatoid arthritis, antibacterial, antifungal, and antiallergic.[12] Among these, the anticancer potential of this pharmacophore has been most widely explored. Chen and coworkers reported a series of 2-aryl-4-benzoyl-imidazoles (ABI) as colchicine-binding-site targeting agents.[13] Courbet et al. reported interactions of EAPB503 with tubulin and their ability to inhibit tubulin polymerization.[14] As synthons, imidazole-based structural scaffolds present many possibilities for structural modification, which has gained the attention of many researchers for the development of new anticancer molecules with diverse improved target specificity and efficiency. Thus, in a continuation of our efforts in developing new anticancer molecules, maintaining the required structural features for the colchicine binding site and taking the lead from previous results, we designed a new series of imidazole-based compounds with various substitution patterns (Figure 1). The series contains imidazole-based fused and non-fused compounds with different substituents at various positions of the imidazole and aryl rings. The designed compounds were synthesized by using a multistep synthetic approach. The synthesized compounds were screened for their cytotoxicity against four cancer cell lines, namely the MCF-7 (breast), MDA-MB-231 (breast), A549 (lung), and HCT-116 (colon) cancer cell lines. In an MTT assay, most the compounds displayed moderate to good activity as compared to the standard drug colchicine. Compounds **P2** and **P5** emerged as the most prominent scaffolds in this series. In mechanistic studies, these compounds displayed similar profiles to colchicine relative to the control and were found to cause apoptosis via cell cycle arrest at the G2/M phase. The results of these studies were encouraging and provide potential lead molecules based on the imidazole scaffold as anticancer compounds.

Results and Discussion

Chemistry

The synthesis of fused imidazoloquinoxaline derivatives is well-reported in the literature.[15] In this work, target molecules were synthesized as shown in Scheme 1. Briefly, diaminomaleonitrile (**1**) was treated with $CH(OEt)_3$ in 1,4-dioxane solvent to afford imidate ester **2**. This was subjected to a substitution reaction with *o*-phenylenediamine to give **3**. In the presence of KOH, **3** underwent cyclization to give 2-aminophenyl-tethered imidazole **4**. Imidazole derivative **4** was treated with appropriate reactants in the presence of *p*-TsOH under different conditions to give the target compounds **P1–5** and **KG1–5**. The synthesized target compounds were purified with chromatography or recrystallization as required. The final characterization of the pure compounds was performed by using mass, IR, and NMR spectroscopic analyses.

Biological Evaluation of Compounds

Cytotoxicity Studies

The synthesized compounds were subjected to MTT assays for evaluation of their cytotoxicity at various concentrations against four cancer cell lines, which included two breast cancer cell lines (MCF-7 and MDA-MB-2321), a lung cancer cell line (A549), and a colon cancer cell line (HCT-116). The MTT method generally evaluates the cellular metabolic activities by measuring the potential of NADPH-dependent cellular oxidoreductase enzymes based on their ability to reduce MTT dye to an insoluble formazan product,

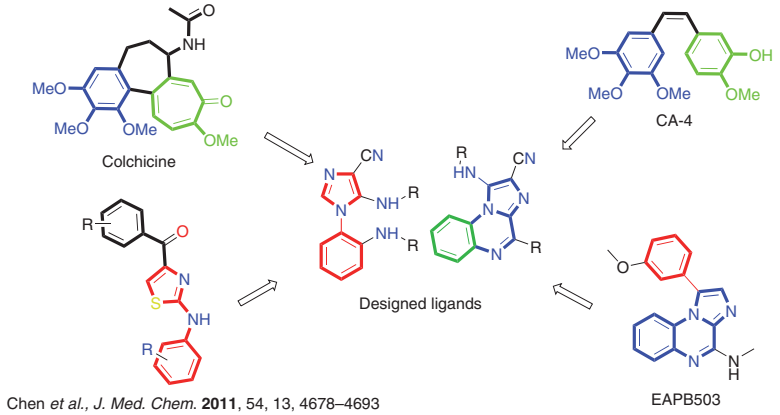

Figure 1 Design of target compounds and their structural features

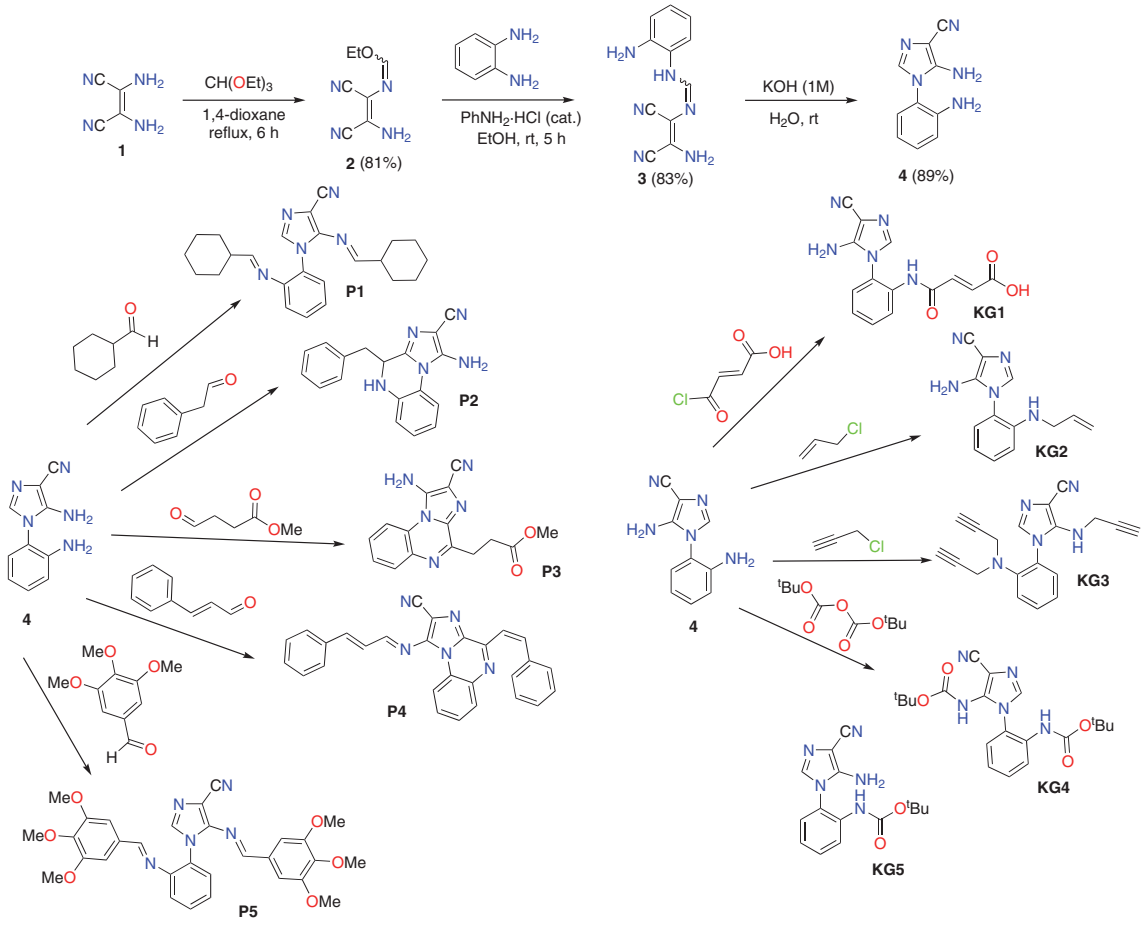

Compound	Mol. Formula	Color	Mp (°C)	% Yield[a]
P1	$C_{24}H_{29}N_5$	Pale yellow	176-178 °C	86
P2	$C_{18}H_{15}N_5$	Yellow orange	177-179 °C	74
P3	$C_{15}H_{13}N_5O_2$	Light yellow	193-195 °C	78
P4	$C_{28}H_{22}N_4$	Pale brown	151-153 °C	69
P5	$C_{30}H_{29}N_5O_6$	Light brown	157-159 °C	73
KG1	$C_{14}H_{11}N_5O_3$	Light brown	201-203 °C	61
KG2	$C_{13}H_{13}N_5$	Greenish yellow	186-188 °C	71
KG3	$C_{18}H_{14}N_6$	Pink	183-185 °C	79
KG4	$C_{20}H_{25}N_5O_4$	Pale brown	205-207 °C	67
KG5	$C_{15}H_{17}N_5O_2$	Yellow orange	191-193 °C	57

Scheme 1 Synthesis of target molecules **P1–5** and **KG1–5**. [a] Isolated yields after purification.

which is purple in color. In these studies, compound **P2** displayed the most potent cytotoxic profile against the MCF-7, MDA-MB-2321, A549, and HCT-116 cell lines with IC_{50} values of 4.34 ± 0.12 µM, 4.73 ± 0.06 µM, 5.21 ± 0.11 µM, and 4.96 ± 0.31 µM, respectively. Similarly, compound **P5**, possessing trimethoxy groups on the benzyl groups attached to the imidazole and aryl moiety, also displayed a balanced profile against these cell lines with cytotoxicity comparable to colchicine. In this series, the compounds with an imidazoloquinoxaline moiety were found to possess better cytotoxicity than other derivatives (non-fused molecules). The compounds with allyl or propargyl substituents at the amino groups of the imidazole and aryl moiety (**KG2** and **KG3**) displayed the weakest activity, and the cytotoxicity was lowered to a large extent. Similarly, compounds with *tert*-butyl carbonate substituents (**KG4** and **KG5**) were also found to have weak cytotoxic profiles relative to those of compounds with fused imidazoloquinoxaline moieties against all four cancer cell lines. The replacement of these substituents with cyclohexane (**P1**) substituents improved the activity to some extent. The results of the MTT studies are presented in Table 1, and they indicate that imidazole-

fused aryl derivatives (imidazoloquinoxalines) can provide optimum pharmacophoric features for developing new anticancer drug molecules against a wide range of cancers.

Table 1 In Vitro Antiproliferative Activity (IC_{50} Value in μM) of Compounds **P1–5** and **KG1–5** against MCF-7, MD-MB-231, A549, and HCT-116 Cancer Cell Lines

Compound	IC_{50} ± S.E.M (μM)			
	MCF-7	MDA-MB-231	A549	HCT-116
P1	8.47 ± 0.32	11.18 ± 0.41	7.68 ± 0.28	9.85 ± 0.18
P2	4.34 ± 0.12	4.73 ± 0.06	5.21 ± 0.11	4.96 ± 0.31
P3	9.12 ± 0.11	7.74 ± 0.21	8.36 ± 0.15	9.53 ± 0.14
P4	13.18 ± 0.52	11.68 ± 0.23	11.26 ± 0.26	16.39 ± 0.25
P5	5.67 ± 0.13	8.18 ± 0.05	7.17 ± 0.15	6.43 ± 0.07
KG1	7.14 ± 0.05	6.11 ± 0.06	6.43 ± 0.14	11.65 ± 0.27
KG2	15.64 ± 0.63	13.18 ± 0.45	17.11 ± 0.17	16.47 ± 0.37
KG3	15.62 ± 0.43	11.46 ± 0.36	13.74 ± 0.53	15.18 ± 0.23
KG4	13.11 ± 0.26	17.37 ± 0.17	14.45 ± 0.24	15.21 ± 0.16
KG5	11.42 ± 0.31	12.32 ± 0.11	8.12 ± 0.07	11.76 ± 0.21
colchicine	5.11 ± 0.33	5.14 ± 0.35	6.55 ± 0.41	5.54 ± 0.33

DPPH Free-Radical Scavenging Assays

The various cellular metabolic activities in our body produce free radicals. Abnormal production of these free radicals plays a significant role in the progression of various diseases, including cancer.[16] The antioxidant activity of compounds, along with their target-specific potential, provides another advantage in anticancer therapy and is hypothesized to lower cancer risks by free-radical scavenging, ultimately lowering the oxidative stress and decreasing abnormal cell division.[17] Thus, to evaluate the free-radical scavenging activity of the synthesized target compounds, DPPH assays were performed at different concentrations (0.01–1 mM). The absorbance of compounds at each concentration, along with the percentage reduction in absorbance (% free-radical scavenging), is displayed in Table 2. The standard antioxidant ascorbic acid was used as a positive control. From the results, it was observed that all of the compounds displayed significant free-radical scavenging activity. The amino groups with a variety of substituents and the cyano groups are thought to play a key role in the free-radical scavenging activity. Compounds **P2–3** and **KG1–5** displayed excellent activity at a concentration of 1 mM. Compound **KG4** containing *tert*-butylcarbonate moieties displayed the most potent free-radical scavenging activity and lowered the free-radical concentration by 35.70%, 49.39%, and 62.40% at concentrations of 0.01 mM, 0.1 mM, and 1 mM, respectively. There was no significant difference in the free-radical scavenging activity of fused and non-fused compounds at higher concentrations. However, compound **P1** showed the lowest free-radical scavenging properties at the lower concentration of 0.01 mM (17.27%). In accordance with the previous literature, this study provides evidence that imidazole-tethered/fused aryl derivatives have significant free-radical scavenging potential, along with their cytotoxic properties, and can be developed as potential anticancer agents with dual target properties.

Table 2 DPPH Free-Radical Scavenging Potential of Synthesized Compounds

Compound	Absorbance at 517 nm (% Reduction in absorbance[a])		
	0.01 mM	0.1 mM	1 mM
control	0.689	0.689	0.689
ascorbic acid	0.365 (47.02)	0.289 (58.05)	0.189 (72.56)
P1	0.570 (17.27)	0.450 (34.68)	0.300 (56.45)
P2	0.460 (33.23)	0.438 (36.42)	0.280 (59.36)
P3	0.436 (33.81)	0.443 (35.70)	0.279 (59.50)
P4	0.430 (37.59)	0.402 (41.65)	0.290 (57.91)
P5	0.480 (30.33)	0.400 (41.94)	0.302 (56.16)
KG1	0.435 (36.89)	0.320 (53.55)	0.240 (65.16)
KG2	0.426 (38.17)	0.401 (41.79)	0.285 (58.63)
KG3	0.459 (33.39)	0.370 (46.29)	0.285 (58.63)
KG4	0.443 (35.70)	0.390 (49.39)	0.259 (62.40)
KG5	0.470 (31.78)	0.398 (42.23)	0.280 (59.36)

[a] % Reduction in absorbance = $(Abs_{control} - Abs_{test})/Abs_{control} \times 100$

Tubulin Polymerization Inhibition Assays

As described in the Introduction, the design strategy involves the design of imidazole-tethered/fused aryl derivatives targeting tubulin polymerization based on the mechanism of action of colchicine and other combretastatin-based derivatives reported in the literature. Thus, the designed cytotoxic compounds were expected to bind to tubulin and inhibit the tubulin polymerization of the arrest cell cycle at the G2/M phase. To confirm the hypotheses and the results from the studies mentioned above, the most active compounds of the series, that is, **P2** and **P5**, were subjected to tubulin polymerization assays. In these studies, the tubulin polymerization inhibition of these compounds was evaluated against bovine tubulin in the absence or

presence (10 µM) of these compounds and colchicine (positive control), and results were recorded over the time period of 2.5 h.

The assays displayed encouraging results (Figure 2A), and both compounds displayed a similar profile to colchicine relative to the control. Both **P2** and **P5** were found to inhibit the polymerization of tubulin in a cell-free system. The process of polymerization was monitored by the measurement of the fluorescence in the presence of the investigated compounds. The treatment dose of both **P2** and **P5** was found to decrease the rate of microtubule formation. Compound **P5** gave a similar result to that of colchicine and displayed good tubulin polymerization inhibition.

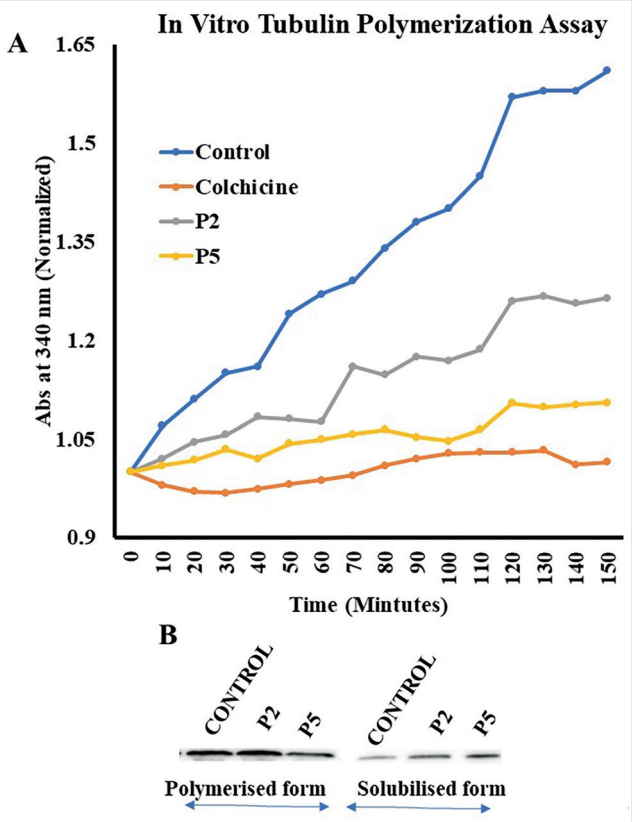

Figure 2 (A) Tubulin polymerization inhibition study of compounds **P2** and **P5** along with colchicine at 10 µM concentration; (B) alteration in the level of solubilized and polymerized tubulin fractions obtained from MDA-MB-231 cells previously treated with a dose of 5 µM and incubated for 24 h

Next, we attempted to quantify the tubulin inhibition of the investigated compounds **P2** and **P5** by obtaining the inhibitory rate. The inhibitory rate was calculated as the fraction of the fluorescence change observed upon treatment with the investigated compound relative to the fluorescence change of the control. The IC_{50} values of **P2** and **P5** were found to be 0.244 and 0.139 nM, respectively, against tubulin polymerization; that of colchicine was 0.203 nM. Furthermore, to obtain better insight, we performed immunoblotting analysis with an anti-tubulin antibody by using MDA-MB-231 cells that were lysed following a 24 h incubation with **P2** and **P5** to obtain solubilized and polymerized tubulin fractions. Colchicine, which acts as a microtubule-destabilizing agent, is usually associated with a decrease in the fraction of polymerized tubulin followed by an increase in the fraction of soluble tubulin, whereas an opposite trend is observed with paclitaxel, which acts by microtubule stabilization. Our investigation revealed (Figure 2B) that both compounds acted as colchicine mimetics and decreased the fraction of polymerized tubulin and increased the fraction of soluble tubulin; they are thus acting as microtubule-destabilizing agents. Between them, **P5** was found to be a much better microtubule destabilizer than **P2** at a concentration of 5 µM.

Cell Cycle and Cell Death Studies

The most active compounds of the series, that is, **P2** and **P5**, were studied for their effect on the cell cycle. Propidium iodide based cell cycle analysis revealed that the compounds could increase the DNA content in the G2/M phase concerning control. The cell cycle analysis further corroborated the occurrence of tubulin destabilization and revealed a halt in the cell cycle at the G2/M phase relative to the control. The propidium iodide intensity that corresponds to DNA content was found to 3.92% in the G2/M phase for the control, but it was elevated to 5.24% with **P2** and 4.98% with **P5** (Figure 3A). Next, we used a propidium iodide versus annexin-V assay to analyze the synthetic compounds for their mode in precipitating cell death in cancer cells. The analysis (Figure 3B) revealed that the primary mode of cell death was apoptosis with respect to the untreated cells. The re-

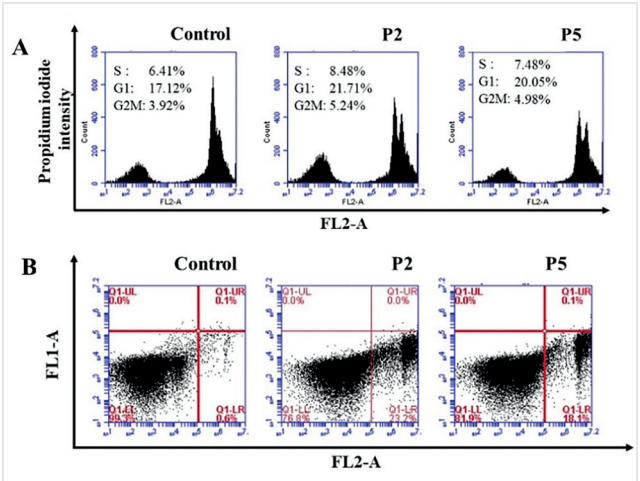

Figure 3 (A) Cell cycle studies with investigated compounds **P2** and **P5** by using propidium iodide; (B) investigation of the mode of cell death by using a propidium iodide vs annexin-V assay. MDA-MB-231 cells were previously treated with the investigated compounds at a dose of 5 µM and incubated for 24 h.

sults obtained from this study, along with the result of cell cycle arrest (at the G2/M phase), indicate that these compounds exhibit anticancer potential through inhibition of tubulin polymerization.

SAR Studies

In the current series, different new imidazole-substituted/fused aryl derivatives were synthesized, and the relationship between their structural features and their pharmacological activity against four cancer cell lines (MCF-7, MDA-MB-231, A549, and HCT-116) was established. Most of the compounds displayed moderate to good cytotoxicity with IC_{50} values in the micromolar range, comparable to those of the standard drug colchicine. A graphical representation of structure–activity relationships is shown in Figure 4.

In Silico Studies

Docking Studies

Molecular docking studies provide insights into a molecule's binding mode and orientation at the binding site of the receptor/enzyme. Thus, to understand the binding mode and interaction pattern, the most potent compounds of the series, **P2** and **P5**, were subjected to molecular docking studies against tubulin protein with co-crystallized colchicine (PDB ID: ISA0) by using Autodock software. The docking protocol was initially validated by re-docking of colchicine at the active site of tubulin, in which the RMSD was found to be well within range, confirming the docking protocol's validation. Compounds **P2** and **P5** displayed better binding scores than the standard tubulin binding agent colchicine, which further confirms the stable binding and

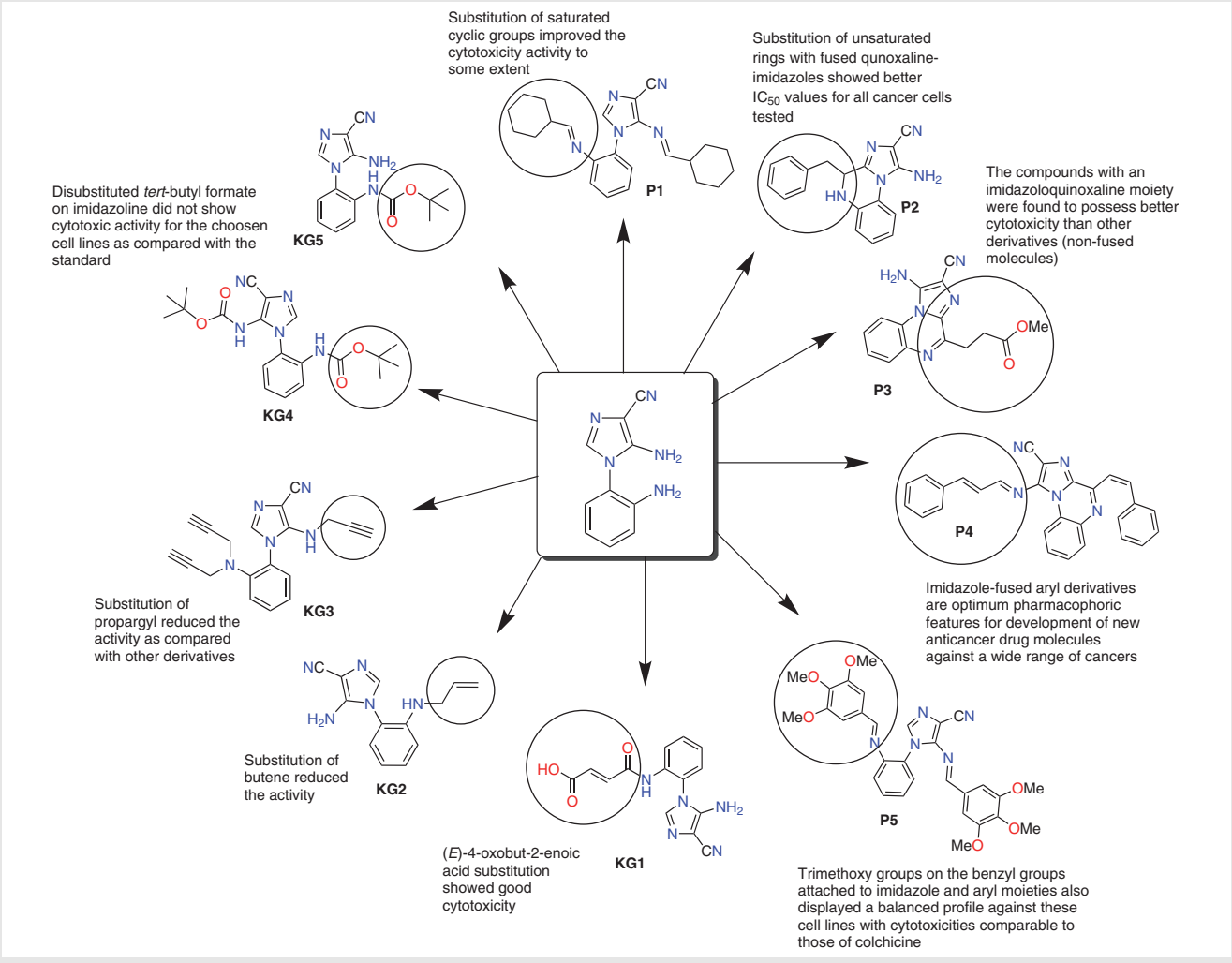

Figure 4 Structure–activity relationship analysis of compounds **P1–5** and **KG1–5**

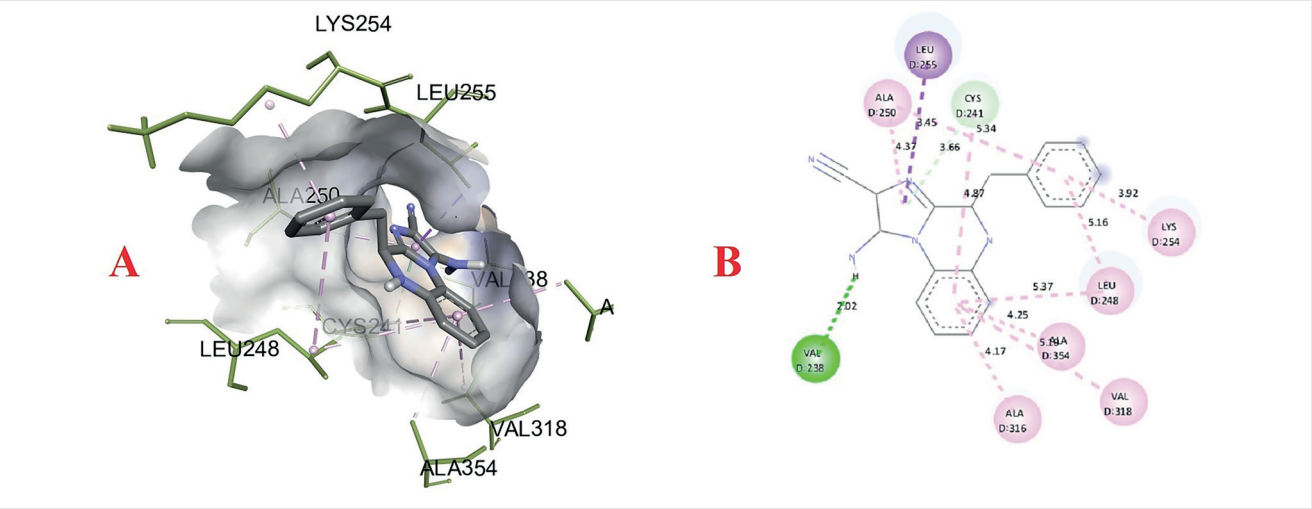

Figure 5 Interactions of compound **P2** with tubulin: (a) 3D interaction pose; (b) 2D interaction pose

good fit of these molecules at the active site of tubulin. Compound **P2** was found to form hydrogen bonding with Val238 (2.02 Å) via the free amino group present at the imidazole ring. It also showed one π–σ interaction each with Ala250 (4.37 Å), Ala316 (4.17 Å), Val318 (5.29 Å), and Ala354 (4.25 Å). There were some additional interactions with the Cys241, Leu248, and Leu265 amino acid residues of tubulin. The 2D and 3D binding patterns are shown in Figure 5.

Similarly, compound **P5** also displayed two hydrogen bonds with Lys352 (2.26 Å and 3.76 Å) via methoxy groups present at the phenyl ring (Figure 6). It formed two π–sulfur bonds with the Cys241 (5.31 Å) and Met259 (5.88 Å) amino acid residues present at the active site of tubulin. It showed various π–alkyl and other hydrophobic interactions at the active site, stabilizing the binding of this compound at the active site. These results were in accordance with the interactions observed in the case of colchicine. Colchicine also formed a hydrogen bond with Lys352 (2.56 Å) via the methoxy group, along with additional π–σ or hydrophobic interactions with various amino acid residues (Figure 7). The findings from these studies are evidence that the synthesized compounds use the same binding pocket and binding pattern. The results also confirm the in vitro observations that these compounds possess similar cytotoxicity and activity against cancer cells to those of colchicine. Therefore, it can be concluded that the title compounds may serve as potential leads for drug development against cancer.

Drug Likeliness, ADME, and Toxicity Predictions

Drug-likeliness studies are performed to predict whether designed or synthesized compounds have drug-like properties. These in silico prediction studies also help predict a compound's bioavailability and pharmacokinetic (ADME) characteristics based on their structural features. If

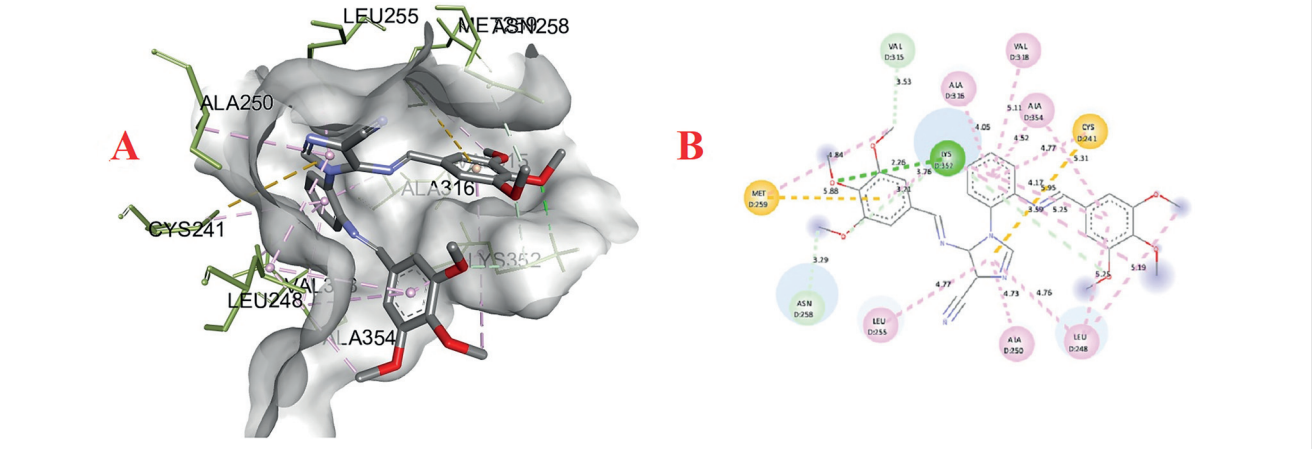

Figure 6 Interactions of compound **P5** with tubulin: (a) 3D interaction pose; (b) 2D interaction pose

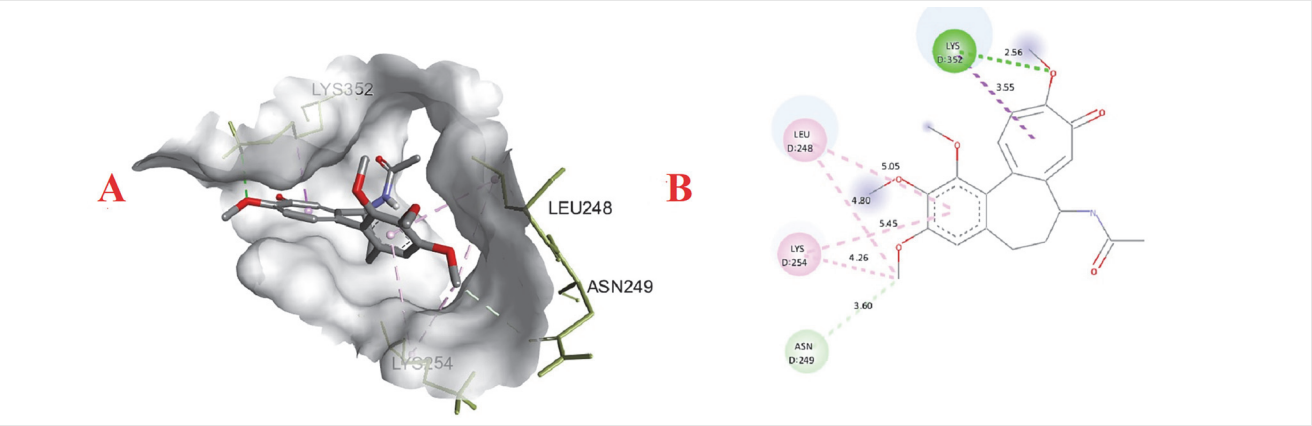

Figure 7 Interactions of colchicine with tubulin: (a) 3D interaction pose; (b) 2D interaction pose

a compound follows Lipinski's Rule of Five, then it is considered to behave as 'drug-like.' As shown in Table 3, the prediction results show that most of the compounds behave like drug molecules and follow Lipinski's Rule of Five. The most potent compounds, **P2** and **P5**, also have good potential to be developed as drug molecules because the molecular weight, Log P, and P_{Caco} values are well in range. The oral bioavailability of compounds **P2** and **P5** is predicted to be 81.52% and 64.02%, respectively. The compounds present a medium risk to the cardiovascular system via acting on HERG receptors. The number of hydrogen-bond donors and acceptors for **P2** is also below five, which further presents this compound as a potential pharmacophore. However, the LogP and P_{Caco} values are on the lower side in between these two compounds. The series **KG1–5** also has moderate drug-like characteristics, and further modifications can be made to develop more potent chemical moieties with drug-like features.

Conclusion

The growing concern about new cancer cases and the rising death toll in the last few decades has increased the zeal to design and develop new anticancer molecules with improved cytotoxicity and target specificity. Tubulin polymerization inhibition is one of the most prominent targets against cancer cells for the development of new chemical moieties. Herein, in a continuation of our efforts to find new anticancer molecules, we report the design and synthesis of imidazole-tethered/fused pharmacologically active aryl derivatives (**P1–5** and **KG1–5**) possessing different substitution patterns targeting tubulin polymerization. The target molecules were synthesized by multistep syntheses and screened for their cytotoxicity against four cancer cell lines. The synthesized compounds displayed moderate to good cytotoxicity, which was comparable to that of colchicine, against all four cancer cell lines (MCF-7, MD-MBA-231, A549, and HCT-116). Compounds **P2** and **P5**, with an imid-

Table 3 Physicochemical Characteristics of Target Compounds

Compound	Mol. weight	$LogP_{o/w}$	HB donor	HB acceptor	P_{Caco}	Percent oral bioavailability	HERG
P1	387.52	3.81	0	4	48.45	86.12	medium risk
P2	301.35	2.53	2	2	10.81	81.52	medium risk
P3	295.30	2.36	1	5	19.02	72.33	low risk
P4	414.50	4.51	0	3	28.27	94.34	low risk
P5	555.58	5.1	0	10	52.55	64.02	medium risk
KG1	297.27	1.35	3	5	18.71	62.76	medium risk
KG2	239.28	2.16	2	2	89.62	81.52	medium risk
KG3	314.34	3.19	3	2	41.05	82.20	medium risk
KG4	399.44	3.47	2	6	17.51	68.20	high risk
KG5	299.33	2.67	2	4	18.58	72.45	medium risk

azoloquinoxaline moiety, emerged as potential leads with cytotoxicity profiles against these cell lines that were similar to that of colchicine. Compounds **P2** and **P5** arrested cell division at the G2/M phase and prevented cancerous cell growth via induced apoptosis. These results favored the hypothesis that the compounds might act by binding to the colchicine binding site, which was further confirmed with the help of a tubulin polymerization inhibition assay. In this study, both compounds showed a similar profile to colchicine. Compound **P5** with a trimethoxybenzene substituent emerged as superior to others in the series. Relative to colchicine, the compounds with other substituents or without ring closure showed low cytotoxicity. These results further encourage the exploration of imidazoloquinoxalines as promising leads that deserve advanced clinical investigation.

N-(2-Amino-1,2-dicyanovinyl)formimydic Acid Ester (2)

The synthesis of *N*-(2-amino-1,2-dicyanovinyl)formimydic acid ester (**2**) was performed according to the procedure reported in the literature.[18] Briefly, a mixture of 2,3-diaminomaleonitrile (3 g) in 1,4-dioxane (20 mL) was placed in a 100 mL round-bottomed flask, and $CH(OEt)_3$ (4.5 mL) was added to it. The resulting mixture was heated to reflux at 80 °C for 6 h, and the reaction was monitored by TLC. After completion of the reaction, the mixture was dried under vacuum by using a rotary evaporator. The brown-colored solid obtained was extracted with diethyl ether (6 × 20 mL) and left overnight at room temperature. Yellow-colored needles of **2** were obtained and utilized for further reactions without any prior purification.

N-(2-Amino-1,2-dicyanovinyl)-N′-(2-aminophenyl)formimidine (3)

N-(2-Amino-1,2-dicyanovinyl)formimydic acid ester (**2**) (3 g, 21.42 mmol) was suspended in methanol (1.5 mL) in a 100 mL round-bottomed flask, and *o*-phenylenediamine (1.85 g, 17.14 mmol) and aniline hydrochloride (2.7 mg, 0.021 mmol) were added in sequence. The resulting mixture was stirred at room temperature for 12 h. The reaction resulted in the formation of precipitates, which were filtered off, washed with diethyl ether, and dried to give **3**.

5-Amino-1-(2-aminophenyl)-1*H*-imidazole-4-carbonitrile (4)

N-(2-Amino-1,2-dicyanovinyl)-N′-(2-aminophenyl)formimidine (**3**) (1 g, 4.42 mmol) was dissolved in water (1 mL), and then 1 M aqueous KOH solution (15 mL) was added. The resulting mixture was stirred at room temperature for 12 h. After completion of the reaction, the mixture was extracted with ethyl acetate (10 mL × 3). The organic layers were combined, washed with water and brine, dried over anhydrous Na_2SO_4, and concentrated under vacuum by using a rotary evaporator to afford the crude product 5-amino-1-(2-aminophenyl)-1*H*-imidazole-4-carbonitrile (**4**). The product's identity was confirmed by using ^{1}H NMR spectroscopy and HRMS.

^{1}H NMR (400 MHz, DMSO-d_6, TMS = 0): δ = 7.21–7.17 (2 H, m), 7.02 (1 H, dd, J_1 = 8, J_2 = 4 Hz), 6.87 (1 H, dd, J_1 = 8, J_2 = 4 Hz), 6.65 (1 H, dt, J_1 = 8, J_2 = 4 Hz), 5.89 (2 H, s, NH_2), 5.15 (2 H, s, NH_2).

HRMS: *m*/*z* calcd for $C_{10}H_9N_5$: 199.0858 [M$^+$]; found: 200.0864 [M + H]$^+$.

P1–5 and KG1–5: General Procedure

A suspension of **4** (100 mg, 0.502 mmol) in methanol (1 mL) was placed in a round-bottomed flask, then different anhydrides/aldehydes (1.004 mmol) and *p*-TsOH (1 mol%) were added. The mixture was stirred at room temperature for 1–2 h. TLC was used to measure the progression of the reaction, and after completion of the reaction, the methanol was evaporated and the mixture was concentrated under vacuum by using a rotary evaporator. The final products were extracted with EtOAc (10 mL × 3), washed with water and brine, dried over anhydrous Na_2SO_4, and concentrated to obtain the crude product. The crude product was purified by flash chromatography or recrystallization as required. The purified products were characterized by using NMR, IR, and mass spectral analyses. The spectral details of new synthetic compounds are provided below.[18]

1-(2-(Allylamino)phenyl)-5-amino-1H-imidazole-4-carbonitrile (KG2)

Yield: 71% (0.29 mmol); greenish-yellow solid; mp 186–188 °C.

IR (KBr): 3395 (NH), 2231 (CN), 1695 (C=O stretch) cm^{-1}.

^{1}H NMR (400 MHz, DMSO-d_6, TMS = 0): δ = 7.23 (1 H, t, J = 8Hz), 7.15 (1 H, s), 6.99 (1 H, dd, J_1 = 8, J_2 = 4 Hz), 6.67 (1 H, dd, J_1 = 8, J_2 = 4 Hz), 6.63 (1 H, dt, J_1 = 8, J_2 = 4 Hz), 5.85 (2 H, s, NH_2), 5.80–5.76 (1 H, m), 5.29 (1 H, t, J = 4 Hz), 5.15 (1 H, dd, J_1 = 12, J_2 = 4 Hz), 5.05–5.02 (1 H, m), 3.68 (2 H, d).

^{13}C NMR (100 MHz, DMSO-d_6, TMS = 0): δ = 148.50, 144.95, 136.25, 134.82, 133.39, 131.08, 129.22, 118.83, 118.09, 116.38, 115.82, 112.63, 90.76, 54.52.

HRMS: *m*/*z* calcd for $C_{13}H_{13}N_5$: 239.1171 [M$^+$]; found: 240.1191 [M + H]$^+$.

1-(2-(Di(prop-2-yn-1-yl)amino)phenyl)-5-(prop-2-yn-1-ylamino)-1*H*-imidazole-4-carbonitrile (KG3)

Yield 79% (0.25 mmol); pink solid; mp 183–185 °C.

IR (KBr): 3385 (NH), 2230 (CN), 1695 (C=O stretch) cm^{-1}.

^{1}H NMR (400 MHz, DMSO-d_6, TMS = 0): δ = 7.32 (1 H, dt, J_1 = 8, J_2 = 4 Hz), 7.14 (1 H, s), 7.02 (1 H, dd, J_1 = 8, J_2 = 4 Hz), 6.88 (1 H, dd, J_1 = 8, J_2 = 4 Hz), 6.72 (1 H, dt, J_1 = 8, J_2 = 4 Hz), 5.82 (2 H, s), 5.53 (1 H, t, J = 4 Hz), 3.83 (2 H, t, J = 4 Hz), 3.29 (4 H, s), 3.03 (1 H, s).

^{13}C NMR (100 MHz, DMSO-d_6, TMS = 0): δ = 146.50, 145.30, 143.80, 139.13, 137.94, 131.51, 129.14, 128.89, 120.08, 117.30, 116.65, 116.07, 113.18, 104.83.

HRMS: *m*/*z* calcd for $C_{19}H_{15}N_5$: 313.1327 [M$^+$]; found: 314.1337 [M + H]$^+$.

tert-Butyl (2-(5-((*tert*-Butoxycarbonyl)amino)-4-cyano-1*H*-imidazol-1-yl)phenyl)carbamate (KG4)

Yield 67% (0.17 mmol); pale brown solid; mp 205–207 °C.

IR (KBr): 3390 (NH), 2229 (CN), 1698 (C=O stretch) cm^{-1}.

^{1}H NMR (400 MHz, DMSO-d_6, TMS = 0): δ = 9.10 (1 H, s, NH), 8.48 (1 H, s, NH), 7.76 (1 H, s), 7.59 (1 H, d, J = 8 Hz), 7.47 (1 H, t, J = 8 Hz), 7.26 (1 H, t, J = 8 Hz), 7.20 (1 H, d, J = 8 Hz), 1.33 (9 H, s), 1.30 (9 H, s).

^{13}C NMR (100 MHz, DMSO-d_6, TMS = 0): δ = 153.45, 153.14, 138.52, 135.26, 130.72, 129.05, 127.50, 125.90, 125.66, 115.39, 107.73, 81.14, 80.03, 28.37, 28.13.

HRMS: *m*/*z* calcd for $C_{20}H_{25}N_5O_4$: 399.1907 [M$^+$]; found: 400.2055 [M + H]$^+$.

tert-Butyl (2-(5-Amino-4-cyano-1*H*-imidazol-1-yl)phenyl)carbamate (KG5)

Yield 57% (0.19 mmol); yellow-orange solid; mp 191–193 °C.

IR (KBr): 3437–3348 (NH_2), 2240 (CN), 1720 (C=O stretch) cm^{-1}.

^1H NMR (400 MHz, DMSO-d_6, TMS = 0): δ = 7.45 (1 H, s, NH), 7.29 (1 H, t, *J* = 8 Hz), 7.08 (1 H, d, *J* = 8 Hz), 6.87 (1 H, t, *J* = 8 Hz), 6.82 (1 H, d, *J* = 8 Hz), 3.87 (2 H, s, NH_2), 1.40 (9 H, s).

^{13}C NMR (100 MHz, *v*, TMS = 0): δ = 152.89, 145.08, 138.71, 136.51, 130.93, 128.68, 118.68, 116.78, 116.62, 115.32, 108.60, 81.08, 28.13.

HRMS: *m*/*z* calcd for $C_{15}H_{17}N_5O_2$: 299.1382 [M^+]; found: 300.1415 [M + H]$^+$.

5-(((*E*)-Cyclohexylmethylene)amino)-1-(2-(((*E*)-cyclohexylmethylene)amino)phenyl)-1*H*-imidazole-4-carbonitrile (P1)

Yield 86% (0.22 mmol); pale yellow solid; mp 176–178 °C.

IR (KBr): 3213 and 3124 (sp^2 hybz C–H stretch), 2237 (CN) cm^{-1}.

^1H NMR (400 MHz, DMSO-d_6, TMS = 0): δ = 8.58 (2 H, d, *J* = 8 Hz), 7.91 (2 H, d, *J* = 8 Hz), 7.63–7.60 (4 H, m), 7.48 (1 H, d, *J* = 8 Hz), 7.12 (1 H, d, *J* = 8 Hz), 2.94 (4 H, d, *J* = 8 Hz), 2.41–2.35 (4 H, m), 0.99–0.85 (12 H, m).

^{13}C NMR (100 MHz, DMSO-d_6, TMS = 0): δ = 152.32, 147.78, 146.23, 145.45, 138.87, 137.63, 136.51, 128.12, 127.38, 125.24, 117.32, 23.45, 22.71, 22.35, 21.98, 21.89.

HRMS: *m*/*z* calcd for $C_{24}H_{29}N_5$: 387.2423 [M^+]; found: 388.2526 [M + H]$^+$.

Methyl 3-(1-Amino-2-cyanoimidazo[1,2-*a*]quinoxalin-4-yl)propanoate (P3)

Yield 78% (0.26 mmol); light yellow solid; mp 193–195 °C.

IR (KBr): 3702 (NH stretch), 3437–3348 (NH_2), 2073 (CN), 1217 (C = N stretch) cm^{-1}.

^1H NMR (400 MHz, $CDCl_3$, TMS = 0): δ = 8.02 (1 H, d, *J* = 8 Hz), 7.96 (1 H, d, *J* = 8 Hz), 7.35–7.27 (2 H, m), 6.37 (2 H, s, NH_2), 4.86 (2 H, t, *J* = 8 Hz), 2.75–2.51 (5 H, m).

^{13}C NMR (100 MHz, $CDCl_3$, TMS = 0): δ = 173.39, 146.78, 141.11, 128.22, 126.87, 126.72, 125.92, 122.14, 118.46, 117.02, 93.76, 53.84, 30.99, 21.85.

HRMS: *m*/*z* calcd for $C_{15}H_{13}N_5O_2$: 295.1069 [M^+]; found: 296.0759 [M + H]$^+$.

Cytotoxicity Studies

The synthesized compounds were subjected to cytotoxic studies using MTT assays as described previously.[19] The MTT method generally evaluates the cellular metabolic activities by measuring the potential of NADPH-dependent cellular oxidoreductase enzymes based on their ability to reduce MTT dye to an insoluble formazan product, which is purple in color. The target compounds were evaluated for their cytotoxicity at various concentrations against four cancer cell lines, which include two breast cancer cell lines (MCF-7 and MDA-MB-2321), a lung cancer cell line (A549), and a colon cancer cell line (HCT-116). The results for the synthesized compounds were compared to those for colchicine, which was used as the standard drug for this series. Briefly, individual cells at a concentration of 1 × 10^4 cells per well were seeded in a 96-well plate and incubated overnight in an incubator for adherence to the surface. After 24 h, the cells were treated with different concentrations of target compounds, with each treatment in triplicate, and cultured for two days in a CO_2 incubator. The medium without any additional compound was used as a control for comparison. After the treatment period, the medium was removed, cells were washed with PBS, and 20 µL of MTT dye solution (5 mg mL^{-1}) was added to each well. After incubation for 4 h, the remaining solution was removed from each well, 100 µL of DMSO was added, and the mixture was left to incubate for 30 min. The DMSO dissolved the formazan formed for measurement of the cytotoxicity of our compounds. The 96-well plate was shaken on a plate shaker, and the absorbance was recorded at 570 nm by using a microplate reader. The results are expressed as IC_{50} values of compounds against each cell line.

Free-Radical Scavenging Assay (DPPH Assay)

The various cellular metabolic activities in our body produce free radicals. The abnormal production of these free radicals plays a significant role in the progression of various diseases, including cancer.[16] Thus, antioxidant activity of compounds, along with target-specific potential, provides another advantage in therapy. Therefore, the synthesized compounds were evaluated for free-radical scavenging activity by using the traditional DPPH (1,1-diphenyl-2-picrylhydrazyl) assay as described previously,[20] with ascorbic acid used as the positive control. Briefly, 3.94 mg of DPPH was accurately weighed and transferred to an amber-colored volumetric flask with a volume of 100 mL. The DPPH was dissolved in 100 mL of methanol, giving rise to a concentration of 0.1 mM. The prepared solution was kept in a dark place for 2 h. Meanwhile, different concentrations of test compounds (0.01–1 mM) in methanol were prepared. To evaluate the free-radical scavenging activity, 2 mL of DPPH solution was mixed with 2 mL of test compound solution. The resulting solution was incubated at room temperature for 30 minutes. After incubation, the absorbance of the resulting solution was measured at 517 nm wavelength by using a UV/visible spectrometer. Each experiment was performed in triplicate, and the results are expressed as the mean of absorbance. The percentage of free-radical scavenging activity was calculated as follows:

Percentage radical scavenging = (A – B) / A × 100

where A = absorbance of control (DPPH) and B = absorbance of sample.

Propidium Iodide vs. Annexin-V Assay

The propidium iodide (PI) vs. annexin-V assay was performed to determine the mode of cell death induced in the MDA-MB-231 cell line after treatment with compounds **P2** and **P5** with respect to the control. The analysis was performed at a 5 µM concentration of the investigated compounds. Briefly, 1 × 10^4 cells were cultured as described previously. Upon confluency, cells were treated with the compounds and were incubated further for 48 h. Thereafter, the cells were washed, the medium (containing debris) was collected, and adhered cells were trypsinized and collected together. The cells were centrifuged and washed thoroughly with 1 × PBS. After being washed, the cells were collected and further incubated with PI and annexin-V dye for 30 min in the dark. After the stipulated time interval, the cells were analyzed by using flow cytometry.

Cell Cycle Study

A similar procedure was followed for cell cycle analysis by using PI. The only difference made was that the cells were fixed before incubation with PI in the dark. The analysis was done by using flow cytometry.

Tubulin Polymerization Inhibition Assay

The tubulin polymerization inhibition assay of the most potent compounds (**P2** and **P5**) was performed against bovine tubulin according to the procedure reported elsewhere.[21] Briefly, the target compounds and colchicine (standard or positive control) were added to 96-well plates in triplicate. Bovine tubulin (1.8 mg mL^{-1}; Sigma) mixed with ice-cold polymerization buffer (PEM: 80 mM PIPES, 0.5 mM EGTA, 2 mM $MgCl_2$, 10% glycerol, and 1mM GTP) was centrifuged for 5 min at 4 °C. After centrifugation, 100 µL of the supernatant were transferred to each well, which already contained the test compounds, colchicine (positive control), or control. After the addition of tubulin, the plate was immediately transferred to the spectrophotometer, which was already maintained at 37 °C. The absorbance was measured at a wavelength of 340 nm every 10 min for 2.5 h. Each experiment was performed in triplicate, and the results are expressed as the mean of these values.

Molecular Docking Studies

To investigate the binding interaction and orientation mode along with the binding energies of the most potent compounds (**P2** and **P5**), molecular docking studies were performed against the tubulin X-ray crystal structure (PDB: 1SA0) by utilizing Autodock software. The 2D structures of the ligands were generated by using the software Chemdraw Ultra 15.0 and prepared by using Autodock Tools version 4.2.6. The 3D structures of the ligands were energy minimized by using Chem 3D Ultra and saved in the pdb format. The X-ray structure of tubulin (PDB: 1SA0) was imported from the protein data bank and prepared by using a sequence of steps, including the incorporation of non-polar hydrogen atoms and the calculation of partial atomic charges by the Kollman method. The protein prepared was saved in pdbqt file format for further use in docking studies. A grid map was generated with grid box dimensions of 34 × 24 × 24 Å at the grid center of 0.375Å. Molecular docking was performed by using Autodock Vina version 1.1.2 via superimposition of the ligands at the grid box, and docking results were obtained as an out file in pdbqt format. The results for docking poses were visualized by using Discovery Studio Visualizer version 17.222 and PyMol Tcl version 1.1. The protocol for molecular docking was also validated by re-docking of the co-crystallized ligand of the imported protein and calculating the RMSD.[22]

Drug Likeliness, ADME, and Toxicity Prediction

Drug-likeliness studies are performed to predict whether the designed or synthesized compounds have drug-like properties or not. These in silico prediction studies also help predict a compound's bioavailability and pharmacokinetic (ADME) characteristics based on the structural features. These properties were predicted by using the online freely available tool SwissADME. Similarly, the toxicity parameters of these compounds were calculated by using the PreADME software, which is freely available online. Furthermore, the ADMET and toxicity properties of the title compounds were determined by using the ProTox-II and PreADME free online software tools.

Conflict of Interest

The authors declare no conflict of interest.

Acknowledgment

All the authors thank their respective affiliated working institutes and universities for providing the necessary infrastructure and support to carry out the current work. K.G. also thanks Prof. Raj Kumar, Professor and Dean, Department of Pharmaceutical Sciences and Natural Products, School of Health Sciences, Central University of Punjab, Bathinda, for his critical feedback and support for the current exploration.

Supporting Information

Supporting information for this article is available online at https://doi.org/10.1055/s-0042-1751835.

References

(1) Joshi, G.; Sharma, M.; Kalra, S.; Gavande, N. S.; Singh, S.; Kumar, R. *Bioorg. Chem.* **2021**, *107*, 104620.
(2) Sung, H.; Ferlay, J.; Siegel, R. L.; Laversanne, M.; Soerjomataram, I.; Jemal, A.; Bray, F. *CA: Cancer J. Clin.* **2021**, *71*, 209.
(3) Kumar, B.; Kumar, R.; Skvortsova, I.; Kumar, V. *Curr. Cancer Drug Targets* **2017**, *17*, 357.
(4) Zich, J.; Hardwick, K. G. *Trends Biochem. Sci.* **2010**, *35*, 18.
(5) (a) Parker, A. L.; Teo, W. S.; McCarroll, J. A.; Kavallaris, M. *Int. J. Mol. Sci.* **2017**, *18*, 1434. (b) Katsetos, C. D.; Herman, M. M.; Mörk, S. J. *Cell Mot. Cytoskeleton* **2003**, *55*, 77. (c) Terry, S.; Ploussard, G.; Allory, Y.; Nicolaiew, N.; Boissiere-Michot, F.; Maille, P.; Kheuang, L.; Coppolani, E.; Ali, A.; Bibeau, F. *Br. J. Cancer* **2009**, *101*, 951.
(6) Pasquier, E.; Kavallaris, M. *IUBMB Life* **2008**, *60*, 165.
(7) (a) Yap, T. A.; Sandhu, S. K.; Workman, P.; De Bono, J. S. *Nat. Rev. Cancer* **2010**, *10*, 514. (b) Nass, S. J.; Rothenberg, M. L.; Pentz, R.; Hricak, H.; Abernethy, A.; Anderson, K.; Gee, A. W.; Harvey, R. D.; Piantadosi, S.; Bertagnolli, M. M. *Nat. Rev. Clin. Oncol.* **2018**, *15*, 777. (c) Wang, R.; Chen, H.; Yan, W.; Zheng, M.; Zhang, T.; Zhang, Y. *Eur. J. Med. Chem.* **2020**, *190*, 112109.
(8) Slobodnick, A.; Shah, B.; Krasnokutsky, S.; Pillinger, M. H. *Rheumatology* **2018**, *57*, 01 i4.
(9) Wilbur, K.; Makowsky, M. *Pharmacotherapy* **2004**, *24*, 1784.
(10) Naaz, F.; Haider, M. R.; Shafi, S.; Yar, M. S. *Eur. J. Med. Chem.* **2019**, *171*, 310.
(11) (a) Kaur, R.; Ranjan Dwivedi, A.; Kumar, B.; Kumar, V. *Anticancer Agents Med. Chem.* **2016**, *16*, 465. (b) Kumar, B.; Singh, S.; Skvortsova, I.; Kumar, V. *Curr. Med. Chem.* **2017**, *24*, 4729.
(12) (a) Luca, L. D. *Curr. Med. Chem.* **2006**, *13*, 1. (b) Sharma, A.; Kumar, V.; Kharb, R.; Kumar, S.; Chander Sharma, P.; Pal Pathak, D. *Curr. Pharm. Des.* **2016**, *22*, 3265. (c) Saccoliti, F.; Madia, V. N.; Tudino, V.; De Leo, A.; Pescatori, L.; Messore, A.; De Vita, D.; Scipione, L.; Brun, R.; Kaiser, M. *J. Med. Chem.* **2019**, *62*, 1330.
(13) Chen, J.; Wang, Z.; Li, C.-M.; Lu, Y.; Vaddady, P. K.; Meibohm, B.; Dalton, J. T.; Miller, D. D.; Li, W. *J. Med. Chem.* **2011**, *54*, 13, 4678.
(14) Courbet, A.; Bec, N.; Constant, C.; Larroque, C.; Pugniere, M.; El Messaoudi, S.; Zghaib, Z.; Khier, S.; Deleuze-Masquefa, C.; Gattacceca, F. *PLoS One* **2017**, *12*, e0182022.
(15) (a) Ammar, Y. A.; El-Sharief, M. A. M. S.; Ghorab, M. M.; Mohamed, Y. A.; Ragab, A.; Abbas, S. Y. *Curr. Org. Synth.* **2016**, *13*, 466. (b) Chen, P.; Iwanowicz, E. J.; Norris, D.; Gu, H. H.; Lin, J.; Moquin, R. V.; Das, J.; Wityak, J.; Spergel, S. H.; De Fex, H.; Pang, S.; Pitt, S.; Shen, D. R.; Schieven, G. L.; Barrish, J. C. *Bioorg. Med. Chem. Lett.* **2002**, *12*, 3153. (c) De Moliner, F.; Hulme, C. *Tetrahedron Lett.* **2012**, *53*, 5787. (d) Gorle, S.; Vaikunta Rao, L.; Chiranjeevi, Y.; Dhanunjaya Rao, A. V.; Mekala, R.; Tadiparthi, K.; Raghunadh, A. *Synth. Commun.* **2022**, *52*, 218. (e) Mamedov, V. A.; Kalinin, A. A. *Russ. Chem. Rev.* **2014**, *83*, 820.

(16) Srivastava, A. R.; Bhatia, R.; Chawla, P. *Bioorg. Chem.* **2019**, *89*, 102993.
(17) (a) Dinkova-Kostova, A. T.; Talalay, P. *Mol. Nutr. Food Res.* **2008**, *52*, 01 S128. (b) Mut-Salud, N.; Álvarez, P. J.; Garrido, J. M.; Carrasco, E.; Aránega, A.; Rodríguez-Serrano, F. *Oxid. Med. Cell. Longev.* **2016**, *2016*, 6719534.
(18) Joshi, G.; Chauhan, M.; Kumar, R.; Thakur, A.; Sharma, S.; Singh, R.; Wani, A. A.; Sharon, A.; Bharatam, P. V.; Kumar, R. *Org. Chem. Front.* **2018**, *5*, 3526.
(19) Kumar, B.; Sharma, P.; Gupta, V. P.; Khullar, M.; Singh, S.; Dogra, N.; Kumar, V. *Bioorg. Chem.* **2018**, *78*, 130.
(20) Kumar, D.; Kumar, R. R.; Pathania, S.; Singh, P. K.; Kalra, S.; Kumar, B. *Bioorg. Chem.* **2021**, *114*, 105068.
(21) Beyer, C. F.; Zhang, N.; Hernandez, R.; Vitale, D.; Lucas, J.; Nguyen, T.; Discafani, C.; Ayral-Kaloustian, S.; Gibbons, J. J. *Cancer Res.* **2008**, *68*, 2292.
(22) Verma, R.; Bhatia, R.; Singh, G.; Kumar, B.; Mehan, S.; Monga, V. *Bioorg. Chem.* **2020**, *101*, 104010.